

DETECTION OF INTRACLUSTER PLANETARY NEBULAE IN THE COMA CLUSTER*

ORTWIN GERHARD¹, MAGDA ARNABOLDI², KENNETH C. FREEMAN³,
NOBUNARI KASHIKAWA⁴, SADANORI OKAMURA⁵, NAOKI YASUDA⁶

Accepted for ApJL, 27-01-2005

ABSTRACT

[OIII] λ 5007Å emission lines of 16 intracluster planetary nebulae candidates in the Coma cluster were detected with a Multi-Slit Imaging Spectroscopy (MSIS) technique using FOCAS on the Subaru telescope. The identification of these faint emission sources as PNe is supported by (i) their point-like flux distribution in both space and wavelength, with tight limits on the continuum flux; (ii) the identification of the second [OIII] λ 4959 line in the only object at high enough velocity that this line too falls into the filter bandpass; (iii) emission line fluxes consistent with PNe at 100 Mpc distance, in the range $2.8 \times 10^{-19} - 1.7 \times 10^{-18} \text{ erg s}^{-1} \text{ cm}^{-2}$; and (iv) a narrow velocity distribution approximately centered on the systemic velocity of the Coma cluster. Comparing with the velocities of galaxies in our field, we conclude that the great majority of these candidates would be intracluster PNe, free floating in the Coma cluster core. Their velocity dispersion is $\sim 760 \text{ km s}^{-1}$, and their mean velocity is lower than that of the galaxies. The velocity distribution suggests that the intracluster stellar population has different dynamics from the galaxies in the Coma cluster core.

Subject headings: (ISM:) planetary nebulae: general; galaxies: cluster: general; galaxies: cluster: individual (Coma cluster); galaxies: evolution

1. INTRODUCTION

Cosmological simulations of structure formation predict that galaxies are dramatically modified by galaxy interactions during the assembly of galaxy clusters, losing a substantial fraction of their stellar mass which today must be in the form of intracluster stars (Murante *et al.* 2004). Observations now show that there is a substantial amount of *intracluster stellar population*, which is observed as diffuse intracluster light (ICL, Bernstein *et al.* 1995), or as individual stars, *i.e.*, planetary nebulae (PNe; Arnaboldi *et al.* 2003, Feldmeier *et al.* 2004) and red giant stars (Durrell *et al.* 2002). The ICL represents about 10% of the stellar mass in the Virgo cluster and as much as 50% in rich Abell clusters (Arnaboldi 2004).

Intracluster planetary nebulae (ICPNe) are the best suited tracers for dynamical studies of the ICL because of their strong [OIII] 5007Å emission, which allows both identification and radial velocity measurement. Measuring the projected phase-space for the ICPNe constrains how and when this light originated (Napolitano *et al.* 2003). So far, ICPNe velocities have been measured only in the Virgo cluster at 15 Mpc distance (Arnaboldi *et al.* 2004). Here we extend these studies to the Coma cluster (Abell 1656), one of the best studied nearby galaxy clusters. Of these, it is the richest and the most compact one, providing a laboratory of prime impor-

tance for studying the effect of a dense environment on galaxy evolution. The ICL in Coma has been suspected since the early study by Zwicky in 1951 and was confirmed by Thuan & Kormendy (1977) and Bernstein *et al.* (1995). The brightest PNe in the Coma cluster at distance of $\simeq 95 \text{ Mpc}$ (Bernstein *et al.* 1995) have fluxes of $2.2 \times 10^{-18} \text{ erg s}^{-1} \text{ cm}^{-2}$ (Ciardullo *et al.* 2002). To detect even the brightest of the Coma PNe, we must find a way to decrease substantially the noise from the night sky.

We can achieve this with a technique that is similar to the approach used by Tran *et al.* (2004) and Martin & Sawicki (2004) to search for Ly α emitting galaxies at very high redshift. It combines a mask of parallel multiple slits with a narrow band filter, centered around the [OIII] λ 5007Å line at the redshift of the Coma cluster, to obtain spectra of all PNe that happen to lie behind the slits. Because the [OIII] emission lines from PNe are only a few km s^{-1} wide, their entire flux still falls into a small number of pixels in the 2D-spectrum, determined by the slitwidth and seeing. On the contrary, the sky emission is dispersed in wavelength, allowing a large increase in signal-to-noise (S/N). The narrow band filter limits the length of the spectra on the CCD, so that more slits can be exposed. For brevity we will refer to this as the Multi Slit Imaging Spectroscopy (MSIS) technique. No conventional imaging technique can decrease the sky surface brightness in a similar way. In this Letter we show that with this technique we are indeed able to detect PNe in the Coma cluster, and briefly describe the first results obtained from one MSIS image in Coma.

2. OBSERVATIONS

The observations were carried out with the FOCAS spectrograph at the 8.2m Subaru telescope on April 23, 2004. The spatial resolution of FOCAS is $0''.1 \text{ pix}^{-1}$, so the 6' diameter of the circular field of view (FOV) corresponds to 3600 pixels. We used grating 300B, which gives a measured dispersion of 1.4–1.5Å per pixel on the two FOCAS CCD chips. We used the N512 filter with FWHM of 60Å, centered at $\lambda_c = 5121\text{Å}$, the wavelength of the redshifted [OIII] emission from a PN at

*BASED ON DATA COLLECTED WITH THE FOCAS SPECTROGRAPH AT THE SUBARU TELESCOPE, WHICH IS OPERATED BY THE NATIONAL ASTRONOMICAL OBSERVATORY OF JAPAN, DURING OBSERVING RUN S04A-024.

¹ Astronomisches Institut der Universitaet, CH-4102 Binningen, Switzerland (ortwin.gerhard@unibas.ch)

² INAF, Oss. Astr. di Torino, Strada Osservatorio 20, 10025 Pino Torinese, Italy (arnaboldi@to.astro.it)

³ RSAA, Mt. Stromlo Observatory, Cotter Road, Weston Creek, ACT 2611, Australia (kcf@mso.anu.edu.au)

⁴ NAOJ, 2-21-1 Osawa, Mitaka, Tokyo, 181-8588, Japan (kashik@zone.mtk.nao.ac.jp)

⁵ Dept. of Astronomy and RESCEU, School of Science, The Univ. of Tokyo, Tokyo 113-0033, Japan (okamura@astron.s.u-tokyo.ac.jp)

⁶ Institute for Cosmic Ray Research, Univ. of Tokyo, Kashiwa, Chiba 277-8582, Japan (yasuda@icrr.u-tokyo.ac.jp)

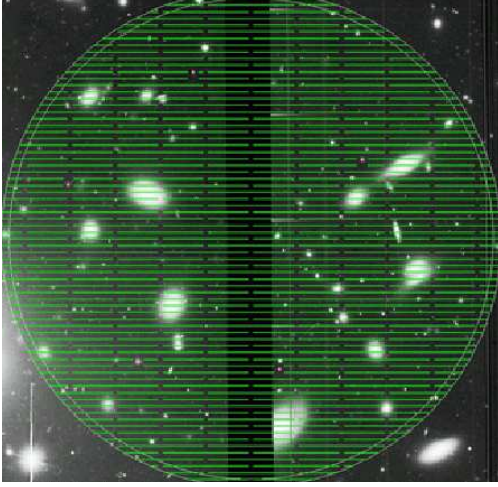


FIG. 1.— Multi-slit mask used in the observations, superposed on the observed field. North is to the left and East is up. The extended light at the NNW margin is from the halo of NGC 4874. The diameter of the FOCAS FOV, indicated by the circles, is $6'$ (about 165 kpc at Coma). The dispersion direction is West-East. Slitlets are arranged along a total of 70 long slits, but with short interruptions for mechanical stability of the mask.

the mean velocity of the Coma cluster. The FWHM includes only $\pm 1.6 \times$ the galaxy velocity dispersion in the Coma core. We will be able to detect the redshifted [OIII] 4959Å emission only for the brighter PNe with the largest receding velocities, $\gtrsim 7400 \text{ km s}^{-1}$, so that it can be seen near the blue edge of the filter.

The light passing through the narrow band filter and a $0''.6$ -wide long slit, and dispersed by the grism projects down to a spectrum of about 43 pixels. A mask was therefore constructed with uniform long slits spaced every 50 pixels, and interrupted only by short sections to ensure mechanical stability (see Fig. 1). The slitlet width on the mask was $0''.6$, corresponding to six $0''.1$ pixels. The area surveyed by this mask configuration is then about $(3600/50)$ slits $\times 0''.6 \times 360'' \times (\pi/4) = 12215 \text{ arcsec}^2$, or 12% of the whole FOCAS FOV.

With this mask, grism, and filter we took six 30 min exposures of a field centered at $\alpha = 12:57:17$, $\delta = +28:09:35$ (B1950). This field is near the X-ray centroid of the Coma cluster and is essentially coincident with the field observed by Bernstein et al. (1995). The measured seeing of the images varied from $0''.6$ to $0''.8$. The CCD readout of the image was done with full spectral resolution and with a spatial binning of 2 pixels. Monochromatic, point-like emitters appear as elongated ellipses on the CCD, with width of approximately 4 rebinned pixels and height of 5 pixels in the wavelength direction. Then the effective spectral resolution is $\simeq 7.3\text{Å}$, or 440 km s^{-1} . Data reduction was carried out in IRAF, with flux calibration using the spectrophotometric standard star BD+33d2642.

2.1. How many PNe do we expect per slit configuration?

We have estimated the average surface brightness of the diffuse light in our Coma core field from the results of Bernstein et al. (1995) to be $R = 24.7 \text{ mag arcsec}^{-2}$. Assuming B-R = 1.0, the average surface brightness in B in this field is 25.7. The total magnitude in the FOCAS circular field of $6'$ diameter is then $B_{TOT} = 13.18$, which amounts to a total luminosity of $L_B = 7.6 \times 10^{10} L_{\odot}$. To estimate the corresponding num-

ber of PNe, we assume that the planetary nebulae luminosity function (PNLF) can be described by the formula of Ciardullo et al. (2002) which is a good fit to numerous observations in nearby galaxies. With the observations described below, we will be complete for PNe $\sim 1.4 \text{ mag}$ fainter than the bright cutoff of the PNLF. Using the luminosity-specific PN density determined for an evolved population such as in M87, $\alpha_{1.0,B} = 5.6 \times 10^{-9} \text{ PN } L_{B,\odot}^{-1}$ (Jacoby et al. 1990, Peletier et al. 1990, Ciardullo et al. 1998), we expect ~ 425 PNe associated with the diffuse light in this field, down to 1 mag fainter than the cutoff.

The fraction of the FOCAS FOV surveyed by the mask used in our observations is 12% (see Section 3), giving about 50 PNe located behind the mask slitlets. However, because the seeing FWHM is nearly equal to the slit width, of order half of these will have a significantly lower flux measured than their true flux; for FWHM=slitwidth, a point source at the center (edge) of the slit is dimmed by 24% (51%). Also, we lose a small fraction of the remaining PNe due to the limited filter bandwidth, if these PNe have the same velocity distribution as the Coma galaxies. Thus finally we expect to detect approximately 20–30 PNe per mask.

2.2. The influence of observational parameters on the detectability of PNe

Here we show how the S/N of the detected PNe depends on the observational parameters, mainly seeing, slit-width, and spectral resolution. For a distance modulus of 34.9, a PN at the bright end of the PNLF has a flux in the [OIII] 5007Å line of $F_{5007,\text{cutoff}} = 2.2 \times 10^{-18} \text{ erg sec}^{-1} \text{ cm}^{-2}$. $0''.6$ resolution corresponds to 300 pc at this distance.

For a sky surface brightness $\mu_V \text{ mag/arcsec}^2$, the magnitude of sky in a pixel $\sigma_x'' \times \sigma_y''$ $m_{v,\text{sky}} = \mu_V - 2.5 \log(\sigma_x \sigma_y)$, and the monochromatic flux from sky at 5500Å in the pixel is $\log F_{\text{sky},\lambda} = -0.4 m_{v,\text{sky}} - 8.4$, or $F_{\text{sky},\lambda} = 4 \times 10^{-9} 10^{-0.4 \mu_V} \sigma_x \sigma_y \text{ erg sec}^{-1} \text{ cm}^{-2} \text{ Å}^{-1}$. For a dispersion d and slit width θ'' , the true spectral resolution is $d_{\text{true}} = d \kappa (\theta / \sigma_y)$, where κ is a constant of order unity. In our observational set-up, the CCD is rebinned 2×1 , giving a spatial resolution $\sigma_x'' \times \sigma_y'' = 0''.2 \times 0''.1$, $d = 1.45 \text{ Å/pixel}$, $\theta'' = 0''.6$, and $\kappa = 5/6$. Thus the flux from the sky surface brightness in the rebinned FOCAS pixel is $f_{\text{sky,pix}} = 4 \times 10^{-9} 10^{-0.4 \mu_V} \sigma_x \sigma_y d_{\text{true}} \text{ erg sec}^{-1} \text{ cm}^{-2}$. For our instrumental set-up, we have measured on the flux-calibrated two-dimensional spectra $f_{\text{sky,pix}} = 7.7 \times 10^{-19} \text{ erg sec}^{-1} \text{ cm}^{-2}$, which gives an effective $\mu_V = 22.2$ at 5120Å , inserting our pixel sizes and spectral resolution.

The PN as a point-like, monochromatic source falls onto $n \simeq \kappa' \pi \phi^2 / (4 \sigma_x \sigma_y)$ pixels, where in our observations the seeing is $\phi = \text{FWHM} = 0''.6$ and $\kappa' = 1.4$. We can thus compute the total signal-to-noise for a PN source. For a total integration time of 3 hrs, i.e. $t_{\text{exp}} = 1.08 \times 10^4 \text{ sec}$, a total telescope area of $S_{\text{tel}} = 5.281 \times 10^5 \text{ cm}^2$, and an overall efficiency of telescope + spectrograph + airmass, $\epsilon = 0.1$, and $h\nu = 3.61 \times 10^{-12} \text{ erg} = E_{5500}$ at $\lambda = 5500\text{Å}$ we obtain

$$\text{SNR}_{PN} = 7.0 \times 10^{-0.4 \Delta m} \quad (1)$$

$$\times \left(\frac{d}{1.45 \text{ Å/pix}} \right)^{-1/2} \left(\frac{\phi}{0''.6} \right)^{-1} \left(\frac{\theta}{6 \sigma_y} \right)^{-1/2} \left(\frac{t_{\text{exp}}}{3 \text{ hrs}} \right)^{1/2}$$

for a PN fainter than the cutoff by Δm magnitudes. Relative to the sky noise in one pixel, the S/N of a PN at the PNLF



FIG. 2.— Two-dimensional median-averaged spectra of emission objects in the FOCAS field. Wavelength is along the vertical axis (507.7–514.15 nm) with a rebinned resolution of 1.5Å per pixel; the true spectral resolution is 7.3Å or 440km s⁻¹. The horizontal direction is along the mask slitlets, with a rebinned resolution of 0.''2 per pixel. The left four panels show PNe candidates from the brightest to one of the faintest in the field. The fluxes are (34.7, 31.9, 18.6, 5.6) ADU, corresponding to (17, 16, 9, 3) × 10⁻¹⁹ erg s⁻¹ cm⁻². The rightmost panel shows the spectrum of a background galaxy with continuum and strong absorption, probably bluewards of Ly α , and a possible line emission, probably Ly α .

cutoff ($\Delta m = 0$) would be 32. Both values assume that the emission from the PN falls through the slit completely. Detection of a source is normally considered to be secure if the S/N relative to the sky noise in one pixel is ≥ 9 . In our data this corresponds to $\text{SNR}_{PN} \geq 2$, i.e., 95% probability of the source being real. If we use this criterion for secure detection, we can detect PNe about 1.4 magnitudes down the PNLF.

Equation (1) shows that independent of all other parameters, good seeing is critical for these observations. Also the SNR_{PN} increases like the inverse square root of the true spectral resolution. However, so that the light of a PN falls through the slitlet completely, we must have $\theta \geq \phi$. Because large slitwidths degrade the spectral resolution, there exists a trade-off between SNR_{PN} and the number of PNe that can be observed through the mask (previous subsection). Consider that the PNLF has a sharp cutoff and then it is nearly flat. Therefore, as long as the SNR_{PN} remains large enough that we can detect PNe one magnitude fainter than the bright cutoff, it is advantageous to use larger slit-widths. For with a larger slit-width, the additional PNe that come through the mask outnumber the PNe that are lost at the faintest fluxes. Typically, to observe one slit configuration for 5–6.5 hours will work as long as the seeing ϕ is not worse than 0.''8.

3. RESULTS AND DISCUSSION: PNE IN THE COMA CLUSTER

A total of 16 spectrally unresolved, point-like sources with undetected continuum were detected on the two CCD chips. Their emission line fluxes were in the range 2.8×10^{-19} – 1.7×10^{-18} erg s⁻¹ cm⁻². Objects with a flux of less than 2.5×10^{-19} erg s⁻¹ cm⁻² (5 ADU) were considered as not real. Figure 2 shows two-dimensional spectra of the two brightest objects, an intermediate flux source, and a low S/N emission. These are all PN candidates. Fig. 2 also shows a source with a possible emission line and a continuum redwards of the line, but no continuum on the blue side, most likely a Ly α -absorbed background galaxy.

We now consider the evidence that the unresolved emission sources are in fact planetary nebulae. Figure 3 shows their 1-d spectra, obtained by summing the respective columns in the 2-d-spectra. The intermediate flux source in Fig. 2 is at sufficiently large recession velocity that, if the observed line

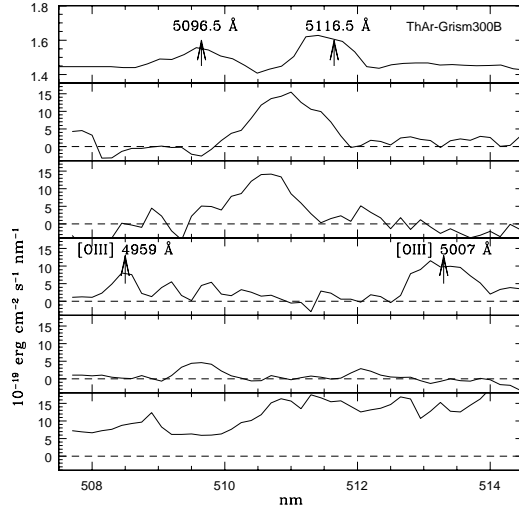


FIG. 3.— One-dimensional spectra of the PNe candidates and of the probable Ly α galaxy shown in Fig. 2 (same order from bottom to top as in Fig. 2). The top panel shows the arclamp image with the two emission lines visible in our spectral range, observed with the same set-up. The widths of the arclamp lines are very similar to the widths of the brighter emission lines of the PNe candidates, showing that these are unresolved in wavelength. The object in the third panel from below is sufficiently redshifted that both lines of the oxygen doublet [OIII] λ 4959Å, λ 5007Å fall in the filter bandpass. The S/N of the emissions from the four PN candidates shown are (20, 18, 11, 3.3) with respect to the noise per pixel of 1.7 ADU or 8.5×10^{-20} erg s⁻¹ cm⁻².

is [OIII] λ 5007Å, the second λ 4959Å line also falls into the narrow band filter. In fact, its 1-d-spectrum in Fig. 3 does show both lines of the doublet: the ratio of the equivalent widths of both lines is consistent with the theoretical value of 1:3.

The brightest object has measured counts of 34.7 ADU in the median image, corresponding to a total line flux of 1.7×10^{-18} erg s⁻¹ cm⁻², and is detected at S/N=20. The faintest PN candidate has a S/N= 3.3, a line flux of 5.6 ADU, corresponding to 2.8×10^{-19} erg s⁻¹ cm⁻², or a total of 68 [OIII] λ 5007Å photons in three hours, about one photon every three minutes. The flux from a PN in Coma at the bright cutoff of the PNLF is 2.2×10^{-18} erg s⁻¹ cm⁻² (Section 2)⁷. Note that our emission sources are generally not centered in the slitlets, and even if they are, we lose 24% (38%) of the flux, given the slitlet width of 0.''6 and a seeing FWHM of 0.''6 (0.''8). Thus the brightest fluxes we measure are consistent with PNe in Coma at the cutoff of the PNLF.

Our candidates are also undetected in the continuum. The 1 σ -upper limit on the pixel flux for the extracted spectra in the range 5070Å–5140Å, excluding the line, is 3.4 ADU, corresponding to a continuum flux limit of 1.6×10^{-20} erg s⁻¹ cm⁻² Å⁻¹. Our brightest object thus has EW>110Å. The V-band continuum flux of an O8 star at the distance of Coma is 4.3×10^{-21} erg s⁻¹ cm⁻² Å⁻¹ – with our observing technique we would see the continuum from a few O stars in the Coma cluster! This rules out compact HII regions such as or brighter than those observed in Virgo (Gerhard *et al.* 2002). Similarly, background galaxies would often have a

⁷ In the [OIII] PNe magnitudes defined by Jacoby (1989) these two objects have $m_{5007} = 30.7$ and $m_{5007} = 32.5$, and the bright cut-off of the PNLF in Coma is at $m_{5007, \text{cutoff}} = -4.5 + 34.9 = 30.4$.

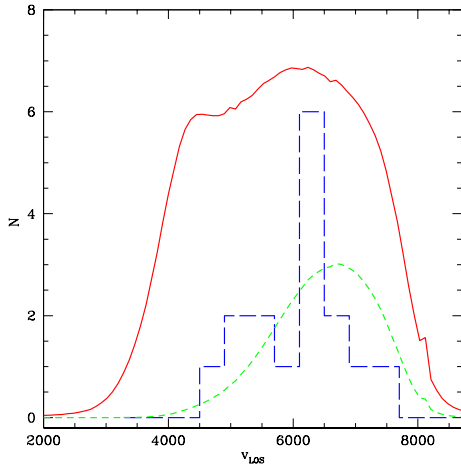


FIG. 4.— Velocity histogram for all 16 PNe candidates in the mask. Mean and median velocities are $\bar{v} = 6100 \text{ km s}^{-1}$ and $v_{\text{med}} = 6224 \text{ km s}^{-1}$, respectively, and the velocity dispersion is $\sigma = 760 \text{ km s}^{-1}$ and $\sigma_{\text{med}} = 562 \text{ km s}^{-1}$ with respect to the median. Overplotted is the measured filter transmission curve in our observing set-up (full red line), using the continuum light from the spectrophotometric standard star BD+33d2642, and (dashed curve) this function times a Gaussian with $\bar{v}_{\text{Coma}} = 6853 \text{ km s}^{-1}$ and $\sigma_{\text{Coma}} = 1082 \text{ km s}^{-1}$ as for the galaxies (Colless & Dunn 1996).

much larger continuum flux than our limit; for example, see the background object shown in Fig. 2. For our brightest candidates, the large equivalent widths are larger than those of known [OII] emitters at $z = 0.37$ (Hogg *et al.* 1998). The line fluxes we measure are 10 - 100 times fainter, and the surface number density is 10 - 100 times higher, than for currently studied Ly α emitters at $z \sim 3$ (Fynbo *et al.* 2003). Moreover, in the flux decade brighter than our brightest line flux, we see no object without measurable continuum, and only one object with blue continuum, for which $\text{EW} = 50 \text{ \AA}$.

Figure 4 shows the velocity histogram for our PNe candidates. They have velocities between $4800 - 7560 \text{ km s}^{-1}$. With our instrumental setup, we detect wavelengths in the range $5071 - 5135 \text{ \AA}$ (FWHM), or velocities in $3830 - 7680 \text{ km s}^{-1}$. The velocity histogram is clearly not uniform in the filter bandpass (Fig. 4); an unclustered population of background emission line galaxies would appear as such a nearly uniform distribution, because only the faintest objects near the filter edges would fall out of the sample.

In summary, we have the following evidence that our unresolved emission sources are PNe in the Coma cluster: (i) They are unresolved both spatially and in wavelength. (ii) They have no detectable continuum, to a limit of $1.6 \times$

$10^{-20} \text{ erg s}^{-1} \text{ cm}^{-2} \text{ \AA}^{-1}$. The brightest object thus has $\text{EW} > 110 \text{ \AA}$. (iii) We have seen both lines of the [OIII] doublet in the only source at sufficiently large recession velocity that also $\lambda 4959 \text{ \AA}$ is redshifted into the wavelength range probed. (iv) The emission fluxes of the brightest objects are consistent with those of the brightest PNe in a population at distance 100 Mpc. (v) The number density of our candidates is consistent with that expected from the measured surface brightness of the ICL in our Coma field. (vi) The distribution of recession velocities is centered around the Coma cluster and is inconsistent with a population of background objects uniformly distributed in velocity. However, we cannot rule out that a population clustered in velocity of so far undetected low-luminosity background emission galaxies could contribute to our sample, if these exist in sufficient numbers at $z \sim 3$ (Ly α) or $z \sim 0.37$ ([OII]).

From Bernstein *et al.* (1995), approximately half of the total luminosity in our field is in the ICL component of the Coma cluster, the other half is in the brighter galaxies, while faint galaxies do not contribute significantly. In the PNe, we expect a larger diffuse light fraction: PNe near bright galaxies will be harder to see because of the increased background. We have superposed our PNe candidates on the image of the field and compared their velocities with those of the brighter galaxies in the field. None of our candidates is close in space and velocity to any of these, but two PNe have measured velocities and positions that could be consistent with the cD envelope of NGC 4874, which is just outside our field, $\sim 120 \text{ kpc}$ from the field center. NGC 4874 itself has a radial velocity of 7224 km s^{-1} and a velocity dispersion of 280 km s^{-1} (Smith *et al.* 2000). Most of our PNe, which have $\bar{v} = 6100 \text{ km s}^{-1}$ and $\sigma = 760 \text{ km s}^{-1}$, are therefore not associated with the halo of NGC 4874.

Thus, the great majority of the detected PNe candidates would be intracluster PNe (ICPNe) in the Coma cluster. It is interesting that the measured mean and dispersion velocities for these ICPNe are smaller than those measured for the Coma cluster core centered around NGC 4874, $\bar{v}_{\text{Coma}} = 6853 \text{ km s}^{-1}$, velocity dispersion $\sigma_{\text{Coma}} = 1082 \text{ km s}^{-1}$ (Colless & Dunn, 1996). A KS test shows that the ICPN velocity distribution has probability 12% to be drawn from the expected velocity distribution of galaxies in our filter (Gaussian times filter band transmission). This suggests that the dynamics of the intracluster population in the Coma core may differ from that of the galaxies, and calls for further investigation.

We acknowledge financial support by the Swiss SNF and by INAF. We are grateful to the on-site Subaru staff for their support.

REFERENCES

- Arnaboldi, M., 2004, in IAU Symp. 217, Recycling intergalactic and interstellar matter, eds. P.A. Duc, J. Brian, E. Brinks, ASP, 54
 Arnaboldi, M. et al. 2003, AJ, 125, 514
 Arnaboldi, M. et al. 2004, ApJ, 614, L33
 Bernstein, G.M., et al. 1995, AJ, 110, 1507
 Ciardullo, R. et al. 1998, ApJ, 492, 62
 Ciardullo, R., et al. 2002, ApJ, 577, 31
 Colless, M., & Dunn, A.M. 1996, ApJ, 458, 435
 Durrell, P. R., Ciardullo, R., Feldmeier, J. J., Jacoby, G. H., & Sigurdsson, S. 2002, ApJ, 570, 119
 Feldmeier, J. J., Ciardullo, R., Jacoby, G. H., & Durrell, P. R. 2004, ApJ, 615, 196
 Gerhard, O., Arnaboldi, M., Freeman, K.C., Okamura, S. 2002, ApJ, 580, L121
 Fynbo, J.P.U., et al. 2003, A&A, 407, 147
 Hogg, D.W., Cohen, J.G., Blandford, R., & Pahre, M.A. 1998, ApJ, 504, 622
 Jacoby, G.H. 1989, ApJ, 339, 39
 Jacoby, G.H., Ciardullo, R., Ford, H.C. 1990, ApJ, 339, 39
 Martin, C.L., & Sawicki, M. 2004, ApJ, 603, 414
 Murante, G. et al. 2004, ApJ, 607, L83
 Napolitano, N.R. et al. 2003, ApJ, 594, 172
 Peletier, R.F., Davies, R.L., Illingworth, G.D., Davis, L.E., Cawson, M. 1990, AJ, 100, 1091
 Smith, R.J., Lucey, J.R., Hudson, M.J., Schlegel, D.J., Davies, R.L. 2000, MNRAS, 313, 469
 Thuan, T.H., Kormendy, J. 1977, PASP, 89, 466
 Tran K.-V., Lilly, S.J., Crampton, D., Brodwin, M. 2004, ApJ, 612, L89